Direct Effects of Lightning on Aircraft Structure: Analysis of the Thermal, Electrical and Mechanical Constraints

L. Chemartin, P. Lalande, B. Peyrou, Arnaud Chazottes, P.Q. Elias, C. Delalondre, B.G. Cheron, F. Lago

L. Chemartin, P. Lalande,
B. Peyrou, A. Chazottes,
P.Q. Elias
(Onera)
C. Delalondre
(EDF)
B.G. Cheron
(Cnrs)
F. Lago
(DGA)

E-mail: laurent.chemartin@onera.fr

Direct Effects of Lightning on Aircraft Structure: Analysis of the Thermal, Electrical and Mechanical Constraints

This paper deals with the direct effects of lightning strike on aircraft structures. In a first part, the phenomenology of lightning arc attachment on aircraft is introduced. Some specific features of lightning arcs observed in flight or created in the laboratory are presented. Some recent developments and results from numerical simulations are shown. The shapes, the behaviors and other specific points are compared with experiments, in order to bring to light some explanations on the complex features of lightning arcs. The second section presents the direct effects of lightning on aircraft skins. Both thermal and mechanical constraints are introduced and illustrated with experimental and numerical results. The negative effects of the paint layer on the damaging of composite and metallic materials are illustrated. The last section is focused on the direct effects of lightning on fasteners. The main mechanisms occurring during sparking phenomena are presented.

Introduction

Lightning strike to aircraft represents a possible safety hazard. The goal of lightning protection is to prevent accidents and increase the reliability of aircraft. The protection of aircraft is based on standards and certification steps [3]. The first step of the certification process, called “zoning”, consists in highlighting the most probable locations of attachment and sweeping zones on the aircraft [31]. Those zones are associated with specific lightning currents. In a second step, structures are tested in the laboratory, under controlled lightning conditions. The physical damages occurring at the attachment point of the lightning arc and, more generally, the damages caused by the conduction of the current into the structure are called “direct effects of lightning”. They can be ascribed either to lightning arcs or to sparks at the surface. The aim of this paper is to investigate the direct effects of lightning arcs on aircraft. The numerical and experimental approaches relevant to this research domain are presented in § "Simulation of lightning arcs". The direct effects on the aircraft skin (wings and fuselage), and on fasteners and assemblies, are respectively presented in § "Lightning direct effects on aircraft skin" and "The direct effects of lightning on fasteners in composites".

Simulation of lightning arcs

Introduction

Industrial and laboratory high power arcs essentially differ from natural lightning ones by their ignition paths. In the former case, the ignition is generally switched on by electric contact (copper wire, mobile electrodes), or by using a high voltage source. In the latter one, high electric strengths in storm clouds lead to the formation and development of streamers, which trigger off the passage to arcs. Another specific feature of lightning arcs concerns the current waveform that travels along them: typically, it consists of a long continuing current on which multiple peaks of current with different amplitudes and shapes are superimposed [1]. A standardized form [2] has been adopted, which involves a sequence of four main current components, called A, B, C and D-waveforms (see figure 1).

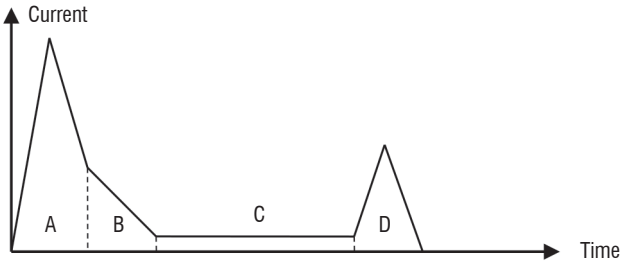

Figure 1 - Standardized lightning current waveforms for lightning direct effect tests (ARP 5412, 2)

These components are related to measured natural lightning currents. The C-waveform is a continuous component. It is associated with the propagation of the lightning discharge in the atmosphere [5]. It can reach hundreds of Amperes with duration of hundreds of milliseconds. The standardized waveform requires a charge transfer of 200 C with current intensities ranging between 200 A and 800 A.

The component A is a high intensity peak. It is followed by an intermediate intensity peak (B). These components are associated with the return stroke phenomena. A-waveform reaches 200 kA with a rise time of a few microseconds and a growth rate of 140 kA/μs. The subsequent stroke (D-waveform) reaches 100 kA with the same rate of rise. A simple bi-exponential formulation is proposed for current components A, B and D [3]:

$$I(t)=I_0\,[e^{-at}-e^{-bt}]$$

This pulse waveform is encountered in RLC electric circuits; it may be used to simulate laboratory capacitive discharge current lightning peaks. Contrary to the evolution described by this equation, measured lightning currents at the ground show a current rate close to zero at the triggering of a return stroke. This data is taken into account by the Heidler waveform [4]. For the sake of comparison, both waveforms are presented in figure 2, together with their rates of rise.

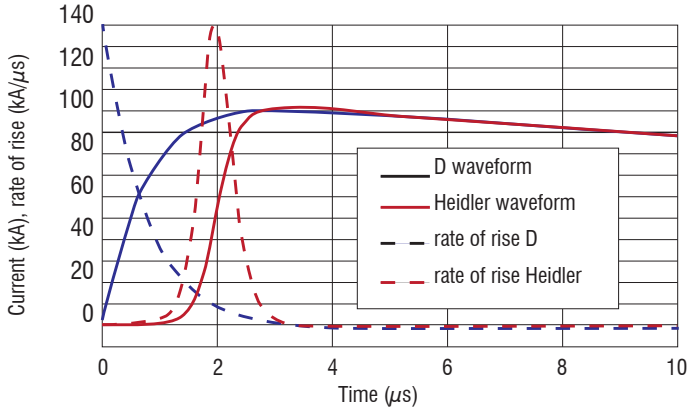

Figure 2 - Comparison of D waveform and Heidler waveform, with their respective rates of rise

International Standard IEC 62305 / European Standard EN 62305 defined return stroke currents with similar shapes. Future lightning waveforms advised in ED-84 [32] documents will take into account this feature.

Transition to thermal arc

The first phase of a lightning strike to an aircraft is associated with the development of a bi-directional leader, which creates the conductive channels. The theoretical analysis of the plasma created by these discharges shows a significant discrepancy between the electron temperature and the heavy particle temperature, due to the high intensity of the electric field necessary for the propagation of the corona [6]. However, once the electric field has decreased enough, elastic collision processes quickly (few microseconds) equilibrate the plasma phases to the same temperature. This transition to LTE (Local Thermodynamical Equilibrium) is an important path in the formation of lightning arcs. The temperature and the electron density in the plasma may be derived from spectroscopic diagnostics by using equilibrium relations (Boltzmann and Saha) and the thermodynamic and transport properties resulting from LTE calculations [7] may be inserted in the set of equations describing the dynamics of the lightning arcs.

Numerical model of lightning arcs

The magneto-hydrodynamic approach (MHD) is one of the ways to simulate the complex dynamics of unsteady electric arcs [8]. In this theoretical frame, the determination of the plasma characteristics requires a set of coupled non-linear equations describing the dynamics of the plasma (Navier-Stokes equations) and the electromagnetic source distributions (Maxwell equations) to be solved. The conservation laws of mass, momentum and total energy of a compressible fluid can be written as:

$$\frac{\partial \rho}{\partial t}+\vec{\nabla}.(\rho\vec{v})=0 \quad (1)$$

$$\frac{\partial \rho\vec{v}}{\partial t}+\vec{\nabla}.(\rho\vec{v}\otimes\vec{v})=-\vec{\nabla}p+\vec{\nabla}.\vec{\tau}+\vec{J}\times\vec{B} \quad (2)$$

$$\frac{\partial \rho e}{\partial t}+\vec{\nabla}\cdot\left((\rho e+p)\vec{v}\right)=\vec{\nabla}.\left(\vec{\tau}\cdot\vec{v}\right)+\vec{J}.\vec{E}-S_{rad} \quad (3)$$

In the above expressions, p, $\vec{v}$, ρ, e and $\vec{\tau}$ are the pressure (Pa), the velocity vector (m/s), the density (kg/m3), the energy per unit mass (J/kg) and the shear stress tensor (Pa) respectively. The momentum $J\times B$ source term is the magnetic force (or Laplace force, N/m3) due to the electric current density J (A/m²) flowing within the lightning channel and inducing a magnetic field $B(T)$. The Joule effect J.E (W/m3) is associated with the heating of the plasma by the current. Ohm's law provides the relationship between the current density J and the electric field E (V/m):

$$\vec{J}=\sigma.\vec{E} \quad (4)$$

Under LTE hypothesis, the electrical conductivity σ (S/m) only depends on the temperature and pressure. The electric field is assumed to play a negligible role in producing free electrons. In the lightning arc and in the aircraft structure, the current distribution satisfies the current conservation equation:

$$\vec{\nabla}\cdot\vec{J}=0 \quad (5)$$

The magnetic field is derived from the Maxwell-Ampere law:

$$\vec{\nabla}\times\vec{B}=\mu_0.\vec{J} \quad (6)$$

In equation 3, S_{rad} (W/m3) is the volumetric radiative power. The accurate calculation of the radiative transfers is a challenging task, due to the spectral, spatial directional and time dependence of the radiation field. Radiative transfers play an important role in high temperature arcs. The volumetric radiative power S_{rad} (W/m3) may be greater than the Joule heating in the constricted regions of the lightning arc and in high intensity pulsed arcs [9], [10]. Several methods have been proposed to calculate this source term. The simplest one is the Net Emission Coefficient, which can be simply tabulated versus temperature. This method quite accurately predicts the temperature level in the hottest part of the plasma, but fails to describe the coldest ones where absorption dominates. Some authors use geometrical methods for accurate calculation of the radiative transfer distribution in the arc (Ray Tracing, P1, Discrete Ordinate Method, etc.). The calculation generally requires a set of spectral bands with averaged absorption coefficients to be selected, in order to avoid huge calculation cost [11].

Simulation of lightning arcs in the laboratory

The direct effects of the lightning arcs are evaluated in the laboratory, using a test set-up advised in the SAE ARP 5416 document [12]. The arc is generated between an electrode and an object under test: generally, a sample of fuselage or wing material (skin) or an assembly. The current generator delivers a specific current waveform associated to the zoning of the structure under test. In the case of a sample associated to fuselage (2A zone), it may be subjected to swept stroke [3]. Thus, the current is composed of D, B and C waveforms. The arc ignition is performed with a thin conductive wire that helps the breakdown in the air gap between the wire and the sample. This electrode is generally a tungsten rod ending in a jet diverter made with a sphere of insulating material. The sphere avoids the test set-up to cause unnatural damages on the surface under test for two main reasons. First, the shock wave associated with current surge is not directed toward the surface. Figure 3 shows indeed the propagation of the pressure wave in the gap between the electrode and the sample 23 μs after ignition. The electrode is above the sample under test. The reflected shockwave close to the sphere is directed towards the sample, but it is relatively low and its intensity decreases with time.

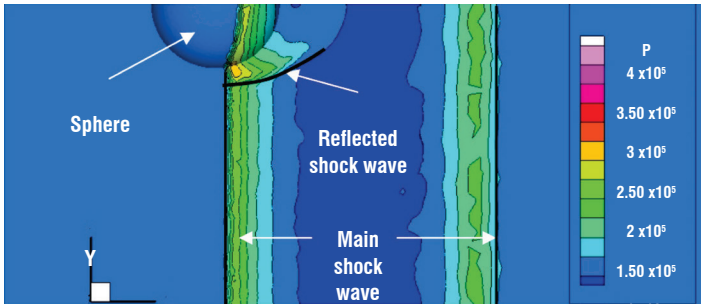

Figure 3 - Formation of shock waves 23μs after ignition with the test set-up advised in the SAE ARP 5416 document

Moreover, the sphere avoids the formation of a jet of plasma directed form the electrode to the sample, as encountered in welding or cutting arcs. Figure 4 shows two laboratory lightning arcs. The electrode is above the test object. The picture on the left was captured by a high speed video camera, 20 ms after the ignition. The current is continuous and its intensity is 800A. The interaction of the plasma jets originating from both electrodes produces instabilities and fluctuations of the arc [13]. The picture on the right was taken with a low shutter speed. The arc is crossed by a surge current of 20 kA. No plasma jet is observed on either of the metallic surfaces due to short time duration of the current pulse. The emissive zone of the arc seems to be more homogenous.

Figure 4 - Left: arc with continuing current of 800A (unpainted aluminum panel, picture DGA-Ta); Right: arc with current surge of 20 kA on copper rod (Onera)

The observation by high speed video cameras helps to understand the complex behaviour of the arc (column and root) during the tests performed with a continuous current wave. One of the most important results derived from video captures is the natural production of a plasma jet on the tested object.

The fluctuations originating from the interaction of the plasma jets during the C-waveform period can be numerically simulated from MHD modeling. Figure 5 shows the results of such calculations for a current intensity set at 800 A, 10 ms after the ignition. The formation of separate plasma jets associated with the highest temperature zones is clearly shown in the picture on the left. These jets result from the strong enhancement of the current density at the electrode interfaces. This constriction of the current streamlines is shown in the picture on the right.

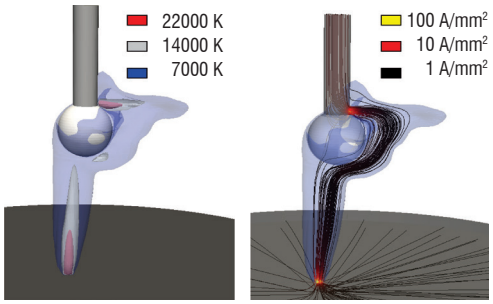

Figure 5 - Left: Calculated isothermal surfaces of an 800 A arc; Right: Calculated current streamlines of an 800 A arc (Onera)

At first, this jet seems to be stable and steady. Then, it is perturbed by the other plasma jet originating from the other electrode. At the panel surface, in the hottest regions, the arc appears to exhibit an axisymmetric brightness profile shape (figure 6, left). In this zone, the numerical simulation highlights a significant increase in the Laplace force resulting from the pinching of the current streamlines, which increases the local pressure and accelerates the plasma outwards. The plasma velocity may reach more than 1000 m/s. We will come back, in the following sections, to the consequences of this high jet constriction on the lightning direct effects on the structure.

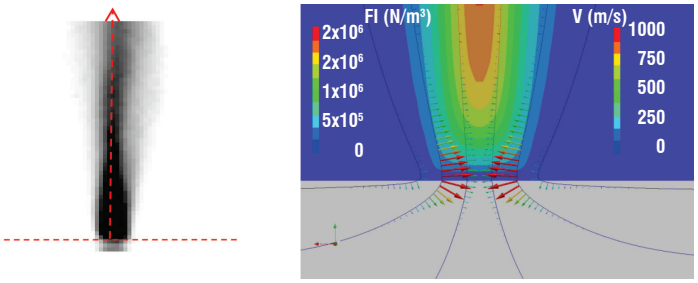

Figure 6 - Left: Picture of the plasma jet at the panel attachment point (DGA-TA) Right, Velocity and Laplace force distributions at the attachment point (Onera)

While the typical radius of an arc attachment with continuing current never exceeds 7mm, numerical investigations on return stroke arcs clearly indicate that this radius continuously expands during the first 100 μs and may reach more than 5 cm for current peaks greater than 100 kA. Since the current density rapidly increases inside the arc (up to 10^9 A/m^2), the temperature quickly increases and reaches 35000 K after a few microseconds. At the same time, the induced Laplace force gives rise to a magnetic pressure with a parabolic shape. This overpressure plays an important role on the dynamics of the arc and on the velocity of the shock wave generated by the return stroke.

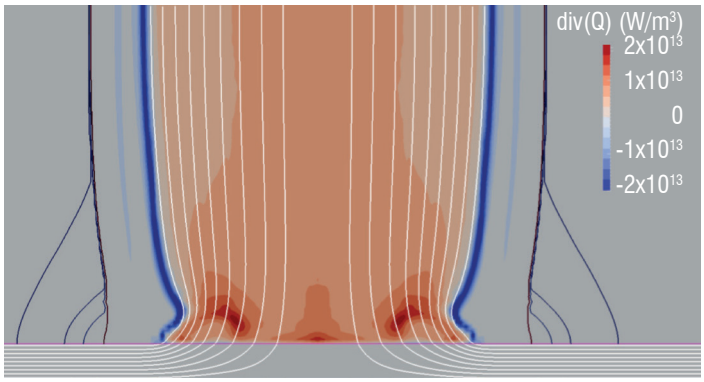

Figure.7 - Color: divergence of the radiative flux (W/m3); White lines: electric current streamlines; Black lines: isobars. (Arc subjected to A/2 waveform at t=10μs on unpainted aluminum panel, Onera)

This overpressure also leads to a significant increase in the radiative emission, which limits the temperature and pressure increase in the core of the arc. On the other hand, the strong energy absorption occurring at the same time in the peripheral regions (blue zones in figure 7) heats the boundary of the arc, the plasma becomes conductive and current flows in this region. Energy absorption is one of the most important mechanisms in the expansion of the arc.

Simulation of lightning strikes in flight

When the lightning strikes happen in flight, the arc is generally more unstable as a result of the aerodynamic flow. A phenomenological description of the swept stroke has been proposed by Larsson et al. [14]. According to this description, the arc root may either dwell at the same spot and follow the fuselage displacement in the air, or continuously sweep the fuselage over small distances. In both cases, the result is a large deformation of the lightning channel and an increase in the electric field in the air gap between the channel and the fuselage (red arrow in figure 8). This electric field is approximately proportional to the length of the channel. When the electric field reaches the critical electric field E_c of the air (about 1 to 3 kV/mm), a dielectric breakdown may happen in the gap. In that case, the arc root jumps from a spot location to a new one. The increase of electric field may be also caused by the natural fluctuation of the arc column, as shown in figure 8.

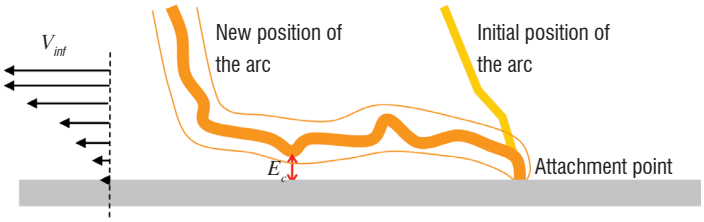

Figure 8 - Schematic drawing of the swept stroke

The objective of the studies dedicated to swept strokes is to characterize the process and to evaluate a dwell time, which is an important parameter for the waveform definition to be applied on the swept zones of aircraft (2 A zone for example). The thermal constraint on the aircraft skin increases as the arc root stays longer at the same point. Some authors have studied the behaviour of the arc sweeping over a structure, using magnetic deflection, wind tunnels [15] or moving structures [16]. They all report a dwell time of a few milliseconds, depending on the fuselage material and on the method used to simulate the swept stroke. These experiments are extremely complicated and they unfortunately do not provide a sufficient collection of data for the engineering.

Such a phenomenon can be simulated by resolving the set of MHD equations presented above. Three important features must be taken into account in the calculation of a swept stroke:

- The natural chaotic behaviour of its long column
- The formation of the plasma jets at the attachment points
- The flow profile along the fuselage, in relation with the aircraft displacement.

Two parameters of the long arc columns greatly influence the reattachment and sweeping processes: the intensity of the internal electric field (or voltage gradient) and the scale of the arc fluctuations. Tanaka et al. [17] have characterized the natural fluctuations of long arc columns by using a high speed imaging technique associated with a reconstruction algorithm. Two values of DC currents were tested: 100 A and 2000 A, with two gap lengths: 1.6 and 3.2 m. These experiments have shown that the motion of the arc columns does not depend on the gap length. Therefore, the role of the electrodes may be neglected in the simulation of such long arcs. Two geometric parameters mainly quantify the tortuosity of the arc: the “expansion radius”, which is the maximum distance from the gap axis reached by the channel, and the “normalized length”, which is the ratio between the effective channel length and the gap value.

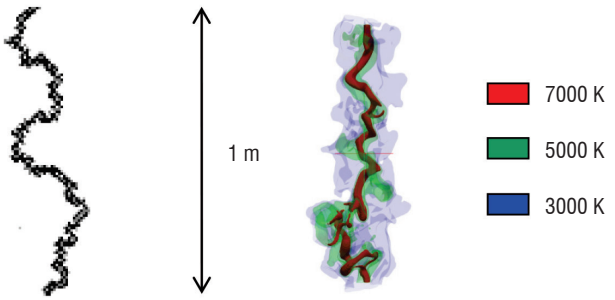

Figure 9 - Behavior of long continuing current arc. Left, picture from Tanaka et al. [17], right simulation [8].

Experiments carried out on long arcs lead to a mean expansion radius of about 10cm for a current of 100 A, with an internal voltage gradient ranging between 500 and 1000 V/m. The normalized length ranges from 1.2 to 1.5. Numerical results [8] quite agree with this experimental data, which validates the use of an electric arc model to simulate the swept stroke. A comparison of the observed and simulated shapes is presented in figure 9

The description by Larson et al. of the sweeping of a lightning stroke was numerically simulated along a simple unpainted panel with a displacement velocity magnitude of 100m/s. Initially, the boundary layer velocity distribution between the panel and the free atmosphere is approximated by means of a Blasius profile extending over 10 to 20 mm. The time of the simulation is 25 ms, corresponding to a panel displacement of 2.5 m. The current is set to 400A. More than 50 reattachments are observed with an expansion radius of about 3 cm around the mean axis of the arc. Figure 10 illustrates a reattachment during the sweeping process. At the time t=11.3 ms, (picture 1), the arc column is slightly extended by the displacement of the skin. The deformation of the column increases with time (picture 2, t=11.85 ms) and the electric field increases between the arc and the panel. This local increase is displayed in picture 10: the blue volume corresponds

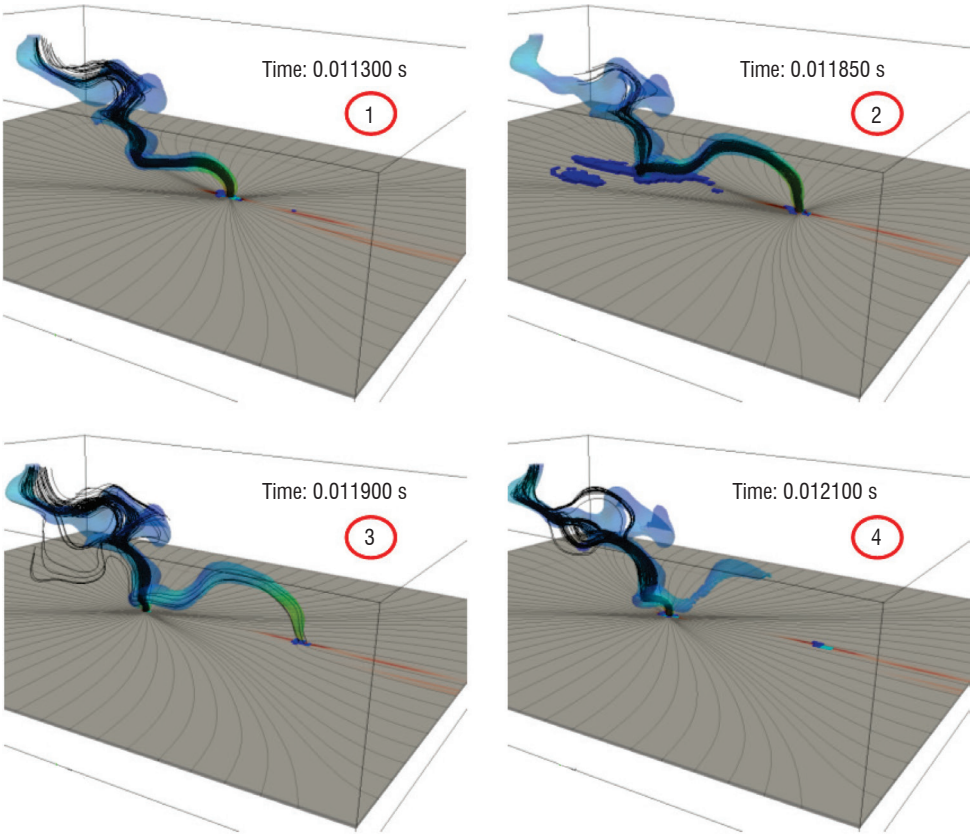

Figure 10 - Simulation of reattachment during the sweeping of a lightning strike along a panel

to a zone in which the electric field amplitude is greater than 0.1 kV/mm. A dielectric breakdown occurs at t=11.9 ms (picture 3) and the arc reattaches in another spot on the panel.

The calculated mean dwell time increases between 0.5 and 3 ms during the sweeping of the arc due to the continuous growth of the boundary layer. These reattachments are associated with quick variations of the voltage, as illustrated in figure 11: four reattachments, with a voltage drop of about 200 V, occur within a 1.5 ms time interval.

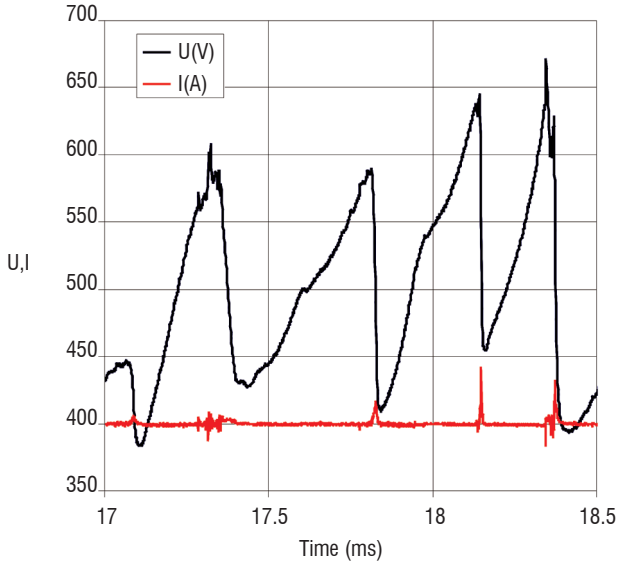

Figure 11 - Evolution of the voltage across the arc during a swept stroke

This evolution of voltage is similar to the voltage measurements of Dobbing & Hanson [16]. It is also similar to the voltage in an argon DC plasma torch in restrike mode [33]. The voltage continuously increases during the lengthening of the arc column and steeply drops at each reattachment. The comparison between a sweeping stroke and a laboratory stationary arc shows that the thermal flux is slightly higher in the former case, while the root radii are in the same order of magnitude. Dobbing & Hanson [16] reported similar conclusions and concluded that laboratory testing with a stationary arc is quite representative of the lightning strike in flight.

Lightning direct effects on aircraft skin

The effects of a lightning strike on aircraft are classified into two main categories: while direct effects are associated with physical damages occurring at the attachment point and in equipment, the indirect effects concern the interferences due to the electromagnetic coupling with the systems and the cabling. This section deals with the direct effects, which are nowadays of primary concern because of the massive use of composite material in the aircraft structure. In a first part, the different mechanisms of damaging are presented. The second part introduces the main physical characteristics of the arc root, and provides the orders of magnitude that define the lightning constraints at the attachment point. The third part presents calculations and measurements of the behaviour of materials struck by the different components of the lightning.

Introduction

The constraints related to direct lightning effects can be divided into two main categories:

The thermal constraints, which are particularly important during the continuing current stage, generate a fast increase in the temperature of the material. They may cause melting or puncture. Some authors have reported empirical linear relationships that give the size of the hole as a function of the total charge transfer and panel thickness [18]. The main energy sources are the direct plasma heat flux (conduction, electronic or ionic recombination and radiation flux) and the Joule heating within the material. In the case of a metal structure, the latter source is negligible due to the high electric conductivity. However, Joule heating may be as important as the flux originating from the plasma in the case of a composite material. Obviously, this difference results from the weak value of the electric conductivity (1000 times lower), but it also comes from the laminate structure of the composite material, which prevents the diffusion of the current through the panel.

The mechanical constraints, which can lead to breaking, delaminating and puncture, are particularly important during the current peaks. The first component of these constraints is the overpressure due to the explosion of the lightning channel, which gives rise to the propagation of a strong shock wave in the radial direction of the arc. The explosion comes from the fast increase in the arc temperature in the channel, up to 30000 K within a time interval of a few microseconds. The magnetic force induced by the current circulation also makes a significant contribution to the mechanical constraint in the arc column and in the material. First of all, the internal pressure of the arc column is reinforced by the concentric magnetic force ("magnetic pinch"): the pressure may reach more than 50 bars within a few microseconds. Furthermore, the current flowing in the structure directly acts as an additional mechanical constraint on the skin ("magnetic pressure"). Finally, the expansion resulting from the very fast increase in temperature of the material yields an additional contribution to the mechanical stress.

Notice that the composite materials are also constrained by the electric field, which can cause internal arcing inside the material and between plies, and lead to the weakening or delaminating of the structure.

The different constraints that occur at the attachment point are shown in figure 12. Different levels of yellows are used in order to feature the arc at different times.

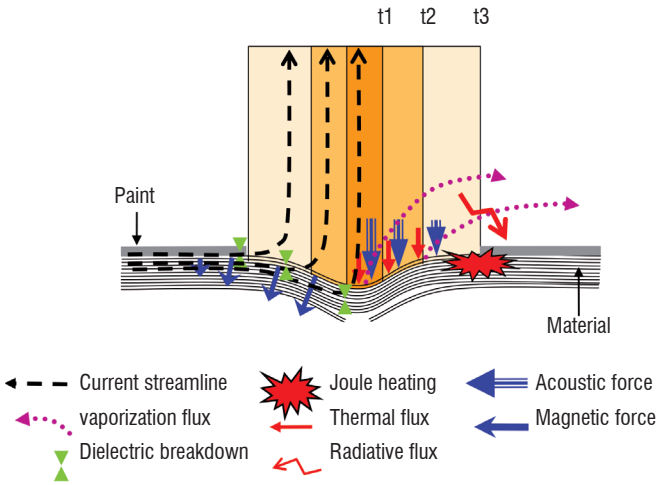

Figure 12 - Illustration of the various direct constraints at the attachment point

The increase in the arc root radius during the lightning stroke highly depends on the surface characteristics of the panel, particularly in the case of paint layers. In the next part, we present various relationships that enable us to assess the various components of the lightning constraints as functions of the arc root radius. These relationships highlight the importance of the radius for the damages. A brief description of various techniques developed to minimize these damages in composite materials is also presented.

Thermal fluxes on arc attachment

The interaction of an arc with an electrode has been widely studied for many years in the context of arc engineering (welding, switching, coating processes, etc.). In the case of lightning strike to aircraft, we can show that the main component of thermal flux is associated with the conduction of the current from the plasma to the structure. The fluxes associated with the vaporizing of the material or radiative emissions are negligible. The physical process involved in the thermal flux depends on the polarity of the material. In the case of an anode, the flux of electrons is directed towards the material, and their acceleration takes place in a thin layer of thickness approximately equal to the mean free path of the electrons (a few μm). The flux component associated with this acceleration is the product of the total current J (A/m²) and an anodic voltage drop noted as U_a (V). When the electrons enter the material, they release some energy and the flux associated with this process is the product of the work function of the material Φ_{Mat} (V) by the total current J. Finally, the conductive flux due to the interaction of neutral particles with the material depends on the plasma temperature T_p and the material temperature T_W. The anodic flux Q_A (W/m²) is generally written as [19]:

$$Q_A = J\left(U_a + \Phi_{Mat} + \frac{5k_b}{2e}\left(T_P - T_W\right)\right)$$

where k_b is the Boltzmann constant and e is the electron electrical charge. The conductive flux is negligible in the case of high current arcs. It is generally considered that both the anodic voltage drop and the material work function are about 4 to 5 V. Thus, a simple relationship of the anodic thermal flux is:

$$Q_A \approx 10\,J \approx 10\,I/\pi R_{c^2}$$

The interaction with a cathode is more complicated because of the thermo-electronic process. When the temperature of the material reaches hundreds of Kelvin, the thermo-electronic emission becomes the main source for the production of electrons. A simple description of the thermal flux between an arc and a cathode consists in considering only thermo-electronic and ionic currents in a mono-atomic and simply ionized plasma layer. With these assumptions, the thermal flux on a cathode Q_K is a function of the thermo-electronic current J_{em} and ionic current J_i :

$$Q_K = -J_{em}\left(\frac{2k_b}{e}T_W + \Phi_{Mat}\right) + J_i\left(\frac{5k_b}{2e}T_W + U_k + \Phi_i\right)$$

Where U_k is the cathode voltage drop (about 10 V), ΦMat is the work function (V) and Φ_i is the ionization potential (13.6 V). The thermo-electronic current is calculated with the Richardson – Dushman formula. An upper bound of the thermal flux on a cathode is:

$$Q_K \approx 24\,J \approx 24\,I/\pi R_{c^2}$$

Thus, it may be considered that the thermal fluxes on both cathode and anode are of the same order of magnitude. While thermal flux relationships with the current density J are linear, the Joule heating depends on the square of the current density (J^2/σ) and the power of

4 of the inverse of the arc root radius. As a conclusion, the thermal constraints highly depend on the radius of the arc root.

Mechanical constraint on arc attachments

The mechanical constraint may be evaluated by the calculation of the magnetic contributions as a function of the radius of the arc attachment. The channel overpressure due to magnetic pinch may be estimated with Newton's first law.

$$\vec{\nabla} p \approx \vec{J} \times \vec{B}$$

The plasma acceleration is neglected and we assume a constant distribution of the current in the arc column of radius R_C. The integration of the pressure along the radius of the channel gives:

$$p_{arc} = \frac{\mu_0 i^2}{4\pi^2 R_C^2}\left[1 - \left(\frac{r}{R_C}\right)^2\right]$$

The contribution of the magnetic force associated with the current drained in the panel may also be decomposed into two contributions. The first contribution is associated with the distribution of the force below the arc root. This force is mainly distributed toward the center (see the right part of figure 6), and the resulting force is necessarily lower than the magnetic pressure of the arc that acts on the panel. This contribution is generally neglected. The second contribution is associated with the outer regions of the arc root [20], [21]. If we consider the same assumptions as before (constant current in the panel and static law), the magnetic pressure is written, for $r > R_C$, as:

$$P_{panel} = \mu_0 i^2 / (4\pi^2 r^2)$$

The sum of both contributions gives the total magnetic pressure acting on the structure, as illustrated in figure 13, for a total current of 100 kA.

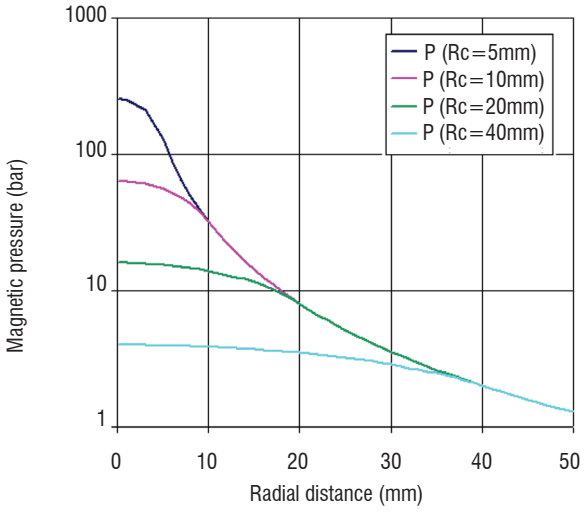

Figure 13 - Distribution of the magnetic pressure at the attachment point for a 100 kA arc

We can see that the maximum pressure reached at the center of the arc column also depends on the inverse of the square of the arc root, as was concluded for the thermal flux.

The acoustic component of the overpressure is due to the fast deposit of energy during the ignition stage of the arc. Some works [22] give some relationships to evaluate the main characteristics of the shock wave after an instantaneous and punctual energy deposit in the case of a perfect gas. The calculation of the fluid flow in the case of a lineic energy deposit indicates that the cylindrical shock position expands with time as a square root law $(R \sim k\sqrt{t})$. This law is proportional to a constant k that takes into account the equivalent energy deposit. The accurate calculation of this energy remains an important issue for the evaluation of the shock wave characteristics with this analytic approach. Numerical modeling and experimental measurements are probably more suitable for the accurate calculation of this component. Such a calculation is presented in the next part, taking into account a more realistic deposit of energy.

Some authors [20], [23] have mentioned the explosion of surface protection as an important contribution to the mechanical stress. This explosion is caused by the strong energy deposit by Joule heating into the thin metal wires of the protection. According to Lepetit et al. [23], the resulting overpressure may reach more than 50 bars.

Characteristics of the arc root

The electric arc model presented in the first section of this paper allows accurate calculations of the characteristics of the arc attachment for the two lightning current components. In the case of the continuing current stage, the goal is to estimate the radius reached at the attachment point. In the case of the current impulses, the model may be used to calculate the evolutions of the arc root radius and total overpressure on the skin.

Characteristics of the arc root during C-waveform

During continuing current tests, observations with high speed video cameras and numerical simulations (figure 6) show that the arc reaches a quasi-steady state shape. Numerical simulations show that the current density profile at the interface with the material reaches a Gaussian like shape (see figure 14). In this condition, it is possible to evaluate a radius R_C into which a given part of the total current flows, for example 99% of the current.

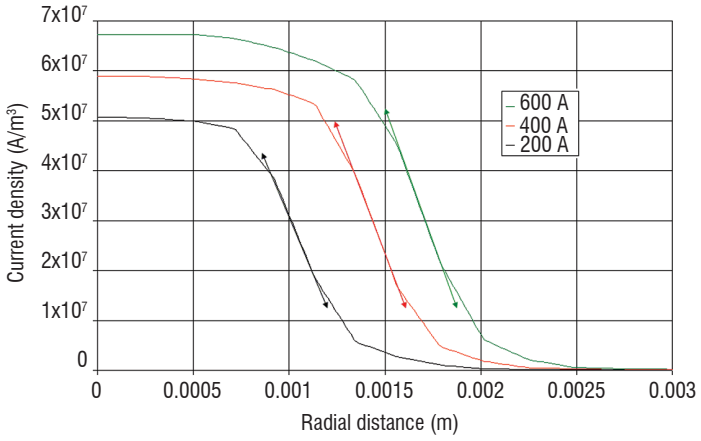

Figure 14 - Calculated distributions of the current at the attachment point during the C waveform

With this assumption, numerical simulations give an equivalent radius of about 1.6 mm for a 200 A arc, 1.8 mm for a 400 A arc and 2.5 mm for an 800 A arc. Thus, the arc root radius depends on the total current that flows into the arc. These values seem to be lower than the

size of the melted zones observed after the tests on material and also the apparent radius evaluated with the analysis of arc pictures. This difference may be explained by the thermal diffusion in the material (see § "Thermal Damaging") which extends the melted zones.

Simulations also indicate that the size of the arc root depends on the presence of a paint layer only during the first 10 milliseconds. After that time, there is no correlation between the presence of the paint layer and the arc root radius. Indeed, the material located around the arc root reaches a temperature above the boiling point in a few milliseconds, while the total duration of the C-waveform is greater than 250 ms. Thus, the paint layer is either vaporized, or carried away by the metal drop (see § "Thermal Damaging").

Characteristics of the arc root during A or D waveforms

While the presence of a paint layer does not affect the arc root radius during the C-waveform, observations of panels after A or D-waveform indicate that the arc root size highly depends on the presence of a paint layer. In the case of an unpainted aluminum panel, the radius of the damaged zone reaches more than 2 cm, while painted panel arc root radii do not exceed 0.5 cm. This feature is illustrated in figure 15, in which the left picture shows the damaged zone of an unpainted aluminum panel tested with a 100 kA arc and the right one shows a painted panel tested under the same conditions.

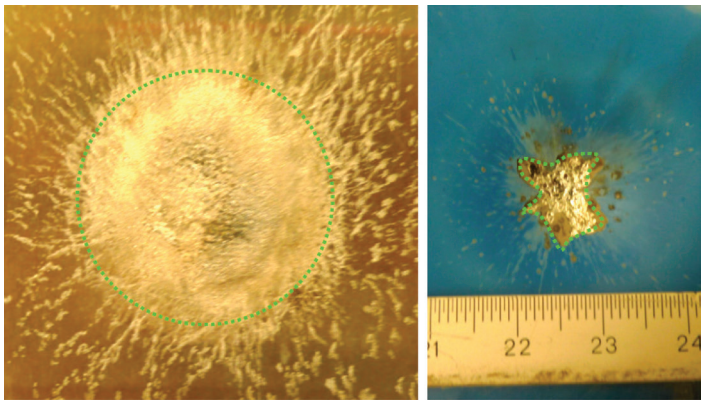

Figure 15 - Pictures of the damaged areas on an aluminum panel after a 100kA lightning test: left on unpainted panel and right with painted panel (same scale).

We can also notice that the damaged area is roughly circular on the unpainted panel, while the shape of the damaged zone on the painted panel is more irregular. A similar analysis of the carbon composite panel may be done, but the action of the protection on the surface is also an important parameter that changes the shape and the size of the damaged zone. Thus, the thermal and mechanical constraints on the panel may be increased by a factor of 10 just because of the presence of a thin paint layer.

Numerical simulations of the arc attachment during the high current stage on unpainted metallic panels show that the arc root continuously expands in the radial direction. This expansion comes from the fluid flows associated with the explosion of the arc and the radiative transfers that heat the surrounding zones of the arc core (see figure 7). During the first 100μs, the arc root characteristics on unpainted aluminum skins are similar to the characteristics of free exploding arcs in air, particularly the temperature and pressure. The results presented in figure 16 concern free exploding arcs in air and provide a good order of magnitude for the interaction of a pulsed arc with an aluminum panel. The current density rapidly increases inside the arc (up to 10^9 A/m^2) and the temperature increases and reaches more than 30000 K within the first microseconds (see figure 16). This deposit of energy leads to the detachment of a shockwave soon after, at about 0.3μs after the arc ignition. This shockwave is associated with an important drop in the pressure, similar to a discontinuity. At the same time, the magnetic force induced by this current density and the magnetic field gives rise to a magnetic pressure with a parabolic shape, as was explained in § "Mechanical constraint on arc attachments". The sum of both contributions gives this typical pressure profile that constrains the skin. The shockwave expansion is faster than the expansion of the conductive zone. However, since the channel radius is expanding and the current starts to decay after 5 μs, the Laplace force and the Joule heating decrease because of the decrease in both the current density and the magnetic field. After 100 μs, the pressure inside the channel is no longer affected by the momentum generated by the Laplace Force.

From this calculation, it is possible to evaluate the expansion of the conductive zone of the arc root, which determines most of the constraints applied on the material. The criterion that defines the equivalent radius of the channel may be defined according to the position of the peak value of the magnetic field in the arc. This criterion gives similar radii to the criteria based on the current content used for continuing current. The evolution over time of this radius R_C is presented in figure 17, with three fit functions associated with three temporal ranges. We can notice that the conducting

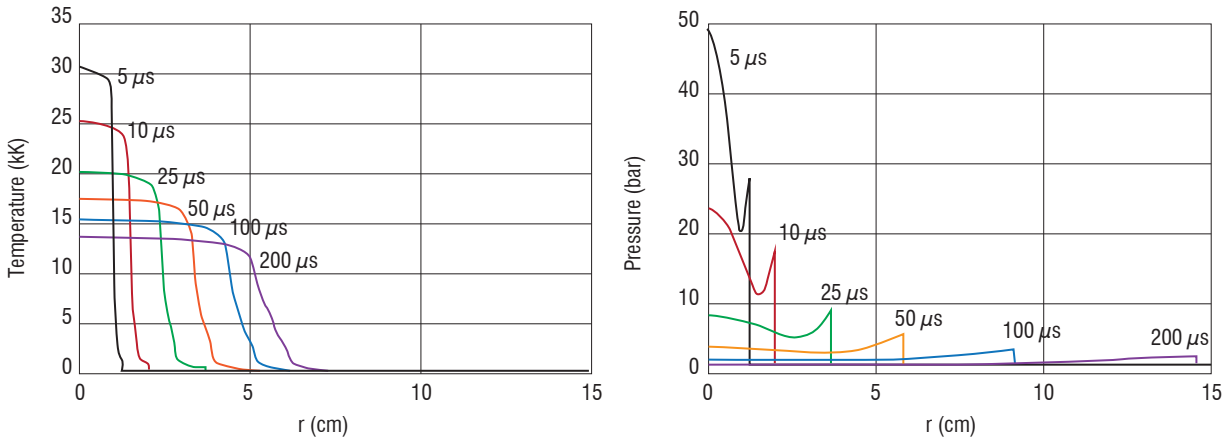

Figure 16 - Distribution of the temperature and pressure at the attachment point during the A/2 waveform

core of the arc expands faster than a pure cylindrical shock wave during the first 20 μs: the fit function during the first tens of μs is a power of 0.57 while the shock radius in a perfect gas expands as a square root. After 50 μs, the conducting core expansion is slower than the pure cylindrical shock (a power of 0.39). This feature may be explained by the fast cooling of the core that increases the density of the plasma and slows down the fluid flow. The effect of the current peak value on the evolution is close to linear. However, as we can observe in figure 17, the expansion velocity decreases with time for all values of the current. The analyses show that the expansion velocity decreases more rapidly when the current is lower. This feature may be explained by the action of the radiative transfers, which plays a very important role in the channel expansion when the current is significant.

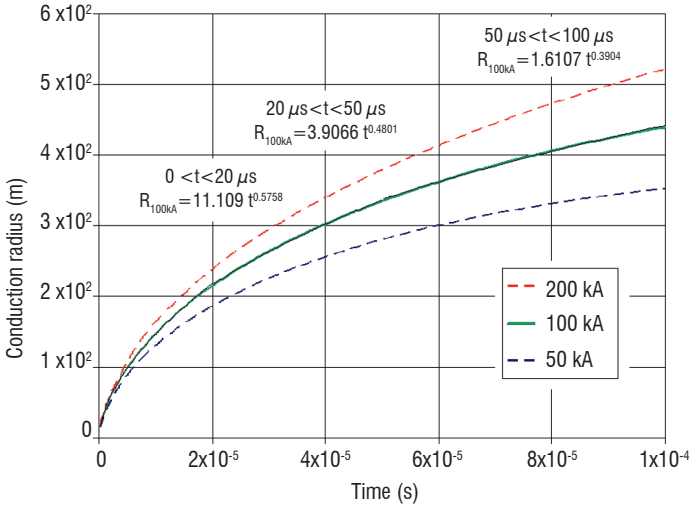

Figure 17 - Evolution of the conductive radius during A/4, A/2 and A waveforms (Onera)

Thermal damaging of aluminum panels during the C-waveform

Observations of continuing arc spots after tests indicate that the areas of melted metal increase with the current value for a same charge transfer [23]. They also indicate that the areas and the depth of the melted zones are more important for cathode polarity [16]. After the test, the spot presents a kind of swelling with a volume greater than the initial state, as illustrated in the two pictures of figure 18 with green dashed lines. This swelling is due to the formation of a molten pool at the arc spot, with air bubbles trapped within. The arc seems to attach onto the top of this swelling and it modifies the shape, as illustrated with red arrows.

Figure 18 - Picture on the left, section through the center of the cathode spot (Dobbing & Hanson, 1978). Picture on the right, view of a cathode spot for an 800A, 200C arc on an aluminum panel (DGA-TA). The drop of metal is deformed by gravity.

This feature highly depends on the metal melting and boiling phenomena and the numerous physical processes involved: metal vapor contamination, surface tension on the molten pool, formation of internal bubbles, etc. Numerical simulations of the arc attachment on such structures are extremely complicated, but some models dedicated to welding engineering give good agreements with observations of arc spots and molten pool formation [24].

Damaging of a carbon composite panel during A or D waveforms

The attachment of the arc on composite panels highly depends on the characteristics of the paint layer and the protection layer. The lightning protection systems are used to prevent composite damage from lightning. These protection subsystems are generally performed with a thin layer of metal located between the ply and the paint layer. A large variety of surface metallization shapes can be used, including expanded copper or aluminum foils (respectively ECF and EAF), solid foil, or bronze mesh (BM). Figure 19 shows two examples of protection used for composites: the left picture is a bronze mesh and the right is an expanded copper foil.

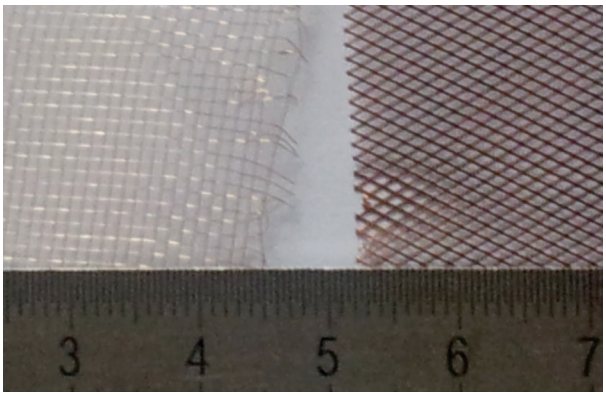

Figure 19 - Left: bronze mesh (BM), right: expanded copper foil (ECF)

This strong interaction between the arc attachment and the surface characteristics (paint and protection system) leads to different types of damaging. The examination of damages after lightning tests indeed shows a large variety of shapes, areas and numbers of damaged plies (see [21]). Areas of damaged protection reported by these authors are greater than 30000 mm² (17 cm wide) on painted panels subjected to an A-waveform (200 kA). They also report areas in which the first ply is seriously damaged with surface damages greater than 3000 mm² (5 cm). Some authors also estimated the delamination area in the composite material using ultrasonic C scan [25] or X ray analysis [26] and they reported a damaged area of thousands of mm². Examples of typical shapes of damaged zones after tests are presented in figure 20, for two types of protection [21]. In these examples, the lightning protection systems are different, but the current component (D) and the paint thicknesses (about 100 μm) are the same for the two panels. In the picture on the left, the protection used is a 65 g/m² Bronze Mesh (BM), while the panel in the picture on the right is protected with a 90 g/m² Expanded Aluminium Foil (EAF).

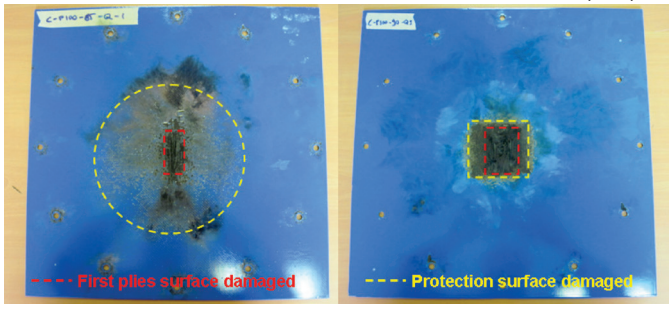

Figure 20 - Picture of the damaged surfaces evaluated for a painted panel protected with BM 65 g/m² (left) and with EAF 90 g/m² (right).(Lago et al. [21])

The EAF 90 g/m² protection seems to be more efficient than the BM 65 g/m² protection in terms of the protection surface damaged. On the other hand, the BM 65 g/m² protection is more efficient than the EAF 90 g/m² if we consider the area in which the first ply is damaged. Experiments show that such a conclusion changes if the waveform, the paint thickness or characteristics of the composite panel change. Thus, it is very difficult to provide a general behavioral law of the arc-panel interaction. Some authors [27] have proposed a classification of the damages as a function of two main types of protection, the paint thickness and the current peak value. For a given paint thickness and a given peak value, the "arc root dispersion" protections (BM 65g/m² for example) give wide and superficial damages while "current conduction" protections (e.g. EAF) are associated with deeper damages over smaller areas.

Numerical simulation may help in the understanding of direct effects of lightning on composite panels. To achieve this goal, all of the processes involved in the damaging must be taken into account. It is also necessary to calculate the distribution of the electric field over the entire integrated panel, in the metallic protection, in the plies, between the plies, and in the paint layer respectively. The current density must be injected into the structure according to the interaction of the arc root with the temporal evolution the surface roughness (presence of paint, metallic protection, resin or composite). The interaction between the vaporization of the protection and the paint layer must be taken into account to correctly simulate the expansion of the arc root. Finally, the dielectric breakdowns between the plies and the pyrolysis of the matrix must be modeled for the calculation of the current distribution in the structure. Such a numerical model is based on many assumptions and cannot pretend to accurately evaluate the damages of a given structure with a given current waveform. However, it provides a qualitative behaviour of the damaging process of a composite panel. The left hand side of figure 21 shows the surface roughness after a 50 kA waveform on a 0.2 cm×10 cm×10 cm carbon stratified panel with a paint layer of 20 μm. The arc attachment radius was set to 1cm. The damaged area is of about 1000mm² and the first ply is not deeply damaged. The right hand side shows the internal state of the panel at t=5 μs for three different paint thicknesses, for a current D waveform. In these simulations, the arc root expands freely according to surface roughness (presence of paint).

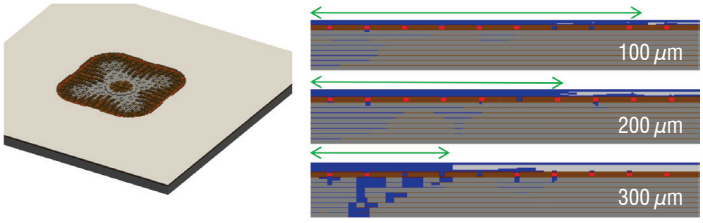

Figure 21 - Left: view of the surface roughness after a 50 kA waveform on a 0.2 cm×10 cm×10 cm carbon stratified panel with a paint layer of 20 μm. Right: cross section of the material at t=5 μs for a D waveform for three different paint thicknesses. (Blue: air plasma, white: paint, red: bronze mesh, brown: resin, grey: ply).

The size of the arc root is visualized with a green arrow on these pictures. We can notice that the arc root radius is greater than 1cm at this time for the 100 μm paint thickness panel while it is about 3.5 mm for the 300 μm paint thickness panel. We can notice that the damages are superficial in the case of the 100 μm paint thickness, while the panel is punctured for a paint thickness of 300 μm. We also notice that several dielectric breakdowns have occurred between the plies (presence of blue layers between the plies). This mechanism is associated with the formation of a conductive path between the plies which gives rise to internal sparking phenomena. Some authors [25] consider that the internal pressure coming from pyrolysis gases accelerates the propagation of the delamination of the stratified material. Internal sparking is an important mechanism in the damaging of composite structure. For the 300 μm paint thickness, the temperature increase in the deep plies is very fast, because the arc root remains small. This leads to a rapid puncture of the panel (t=5 μs). Simulations have shown that foil or expanded metal protections limit the electric field penetration into the material and avoid the breakdowns between deep plies. Moreover, metal meshes involve current reinforcements on each crossing of wires, which give rise to metal vaporization and the rapid decrease in mesh resistance. This mechanism does not exist in metal foil protections because they lead to a continuous current dispersion toward the boundary of the panel.

Mechanical damaging of aluminum and composite panels during stroke

In § "Mechanical constraint on arc attachments" and § "Characteristics of the arc root", the theoretical mechanical force that acts on the panel was presented. The examination of aluminum panels after tests shows a plastic deformation that may reach more than one centimeter. The plastic deformations in composite panels do not appear clearly, probably due to the elastic nature of the composite material. However, the mechanical damage in composite panels is the delaminating phenomena, which require internal analysis (X ray, ultrasonic scan, etc.). Some experimental measurements of the panel displacement during lightning attachment have been performed with various techniques [20], [21] and [28]. They showed transient deflection that evolves as a decaying sine wave, on which some additional modes may be superimposed. Observation of 2D displacements with a digital image correlation technique [21] shows that the deflection of the panel is mainly axisymmetric. These modes are represented in figure 22.

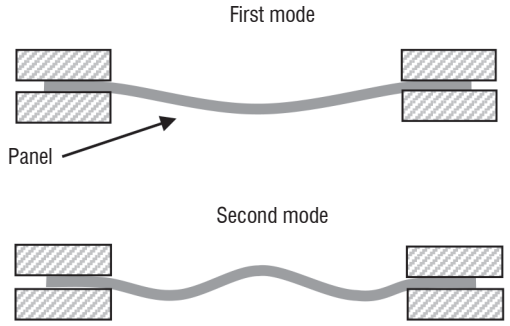

Figure 22 - First and second axisymmetric modes of an embedded panel

Deflection analyses show some important features associated with the mechanical stress that leads to mechanical damage. These have shown that the maximal deflection recorded is proportional to the square root of the action integral. They give some theoretical explanations of this feature, for both aluminum and composite materials. This result allows the correlation of an arc parameter (e.g. the action integral) with the mechanical response (the maximal deflection) of a given sample. Experimental measurements also highlight the fact that the presence of a paint layer increases the deflection of tested panels. For aluminum skins, the paint layer drastically increases the plastic deformation at the attachment point. For composite panels, as is observed for thermal damages, it is more the paint/protection couple

that has an effect on the panel. High current tests (A waveform) with thick painted panel (>300 μm) generally lead to large scale delaminating and mechanical breakdown. It is believed that the mechanical impulse on such panels is the most important constraint.

Simulations of the mechanical response of panels, on which theoretical mechanical stresses evaluated with arc simulations are used, give relatively good agreements with measurements. A transient nonlinear approach is required for this type of simulation. The results indicate that both the magnetic and hydrodynamic pressure must be taken into account to correctly calculate the panel deflection in all types of material, with or without paint. Figure 23 shows a 2D simulation of the deflection of a 2mm thick aluminum panel. The blue zone represents the panel position before the load, and the colored zone represents the panel with lightning load at t=1.4 ms. During this simulation, the maximal deflection is about 1mm. This figure shows the internal Von Mises stress that predicts yielding of materials under the loading condition. We can notice that the stress is maximal at the center of the panel, near the attachment of the arc on both sides of the panel.

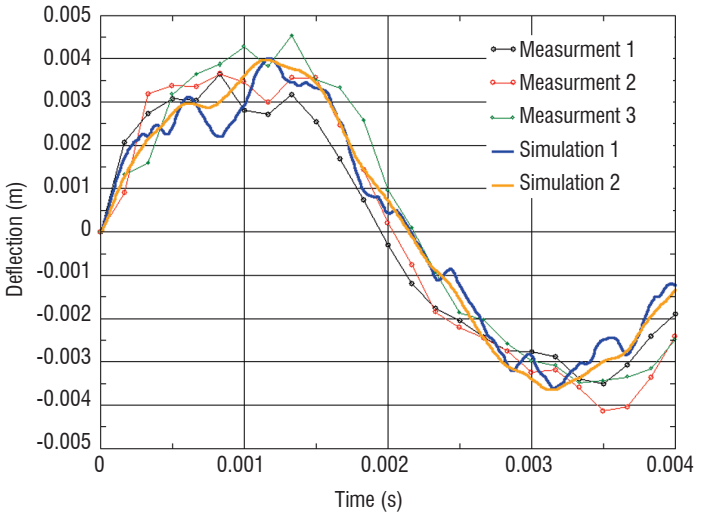

Figure 24 - Evolutions of the measured and simulated deflections of composite panels

Analyses have indicated that the location of the attachment point on the panel does not change either the frequency of the oscillations, or the position of maximal deflection, which is always located at the center of the panel. Moreover, the maximal deflection slightly varies with the location of the attachment point. These conclusions are important because accurate control of the arc root position during testing is not possible. Thus, comparisons of the measured and simulated maximal deflection point on the panel can be performed. Figure 24 shows the changes in the measured deflection at the center of the panel, for three composite panels subjected to a D waveform. The changes in deflection calculated with mechanical software are also plotted with bold continuous lines. The loading associated with this deflection is a sum of the magnetic pressure presented in § "Mechanical constraint on arc attachments" with an analytic model of shock wave propagation. Two values of equivalent radius Rc have been used: the lowest value corresponds to “Simulation 1” and the highest to “Simulation 2”. We can notice a relatively good agreement with measurements on the rise time and the maximum deflection.

More generally, numerical and experimental analyses indicate that the deflection of unpainted panels (composite and aluminum) is mostly due to the acoustic shock wave, while painted panels seem to be more stressed because the magnetic pressure acts as an additional contribution. More specifically, the large plastic deformation in painted aluminum panels cannot be simulated without taking into account the contribution of magnetic pressure over a small area of 8 to 10 mm radius.

The direct effects of lightning on fasteners in composites

Introduction

The massive use of composite materials in modern aircraft requires careful consideration regarding how the lightning strike attaches and how the current flows through the structure. The great difference between the electric conductivity of metallic fasteners and the conductivity of composite materials increases the probability of lightning attachments to fasteners. Moreover, the large number of fasteners used in aircraft

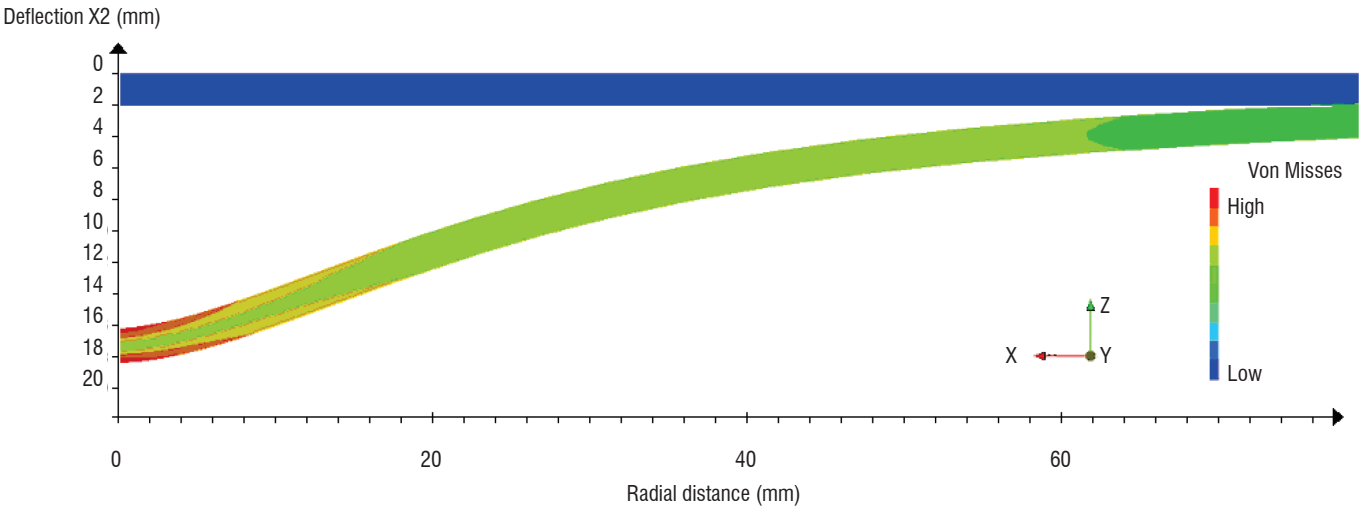

Figure 23 - Deflection of the panel. Color: Von Mises criteria

construction creates conditions for the current to flow through fasteners by conduction in distant zones of attachment. Sparking or arcing phenomena are generally observed on fasteners in which a strong current flows, with likely hazardous effects in the fuel tank area.

Phenomenology

The direct effects of lightning on fasteners and rivets are generally the source of several physical mechanisms. The occurrence of these mechanisms depends on the material used for the assembly (for example, metal rib with carbon composite), the type of electrical threat (attachment or conduction) and the value of the current peak. In the following sketch (figure 25), we present the three main mechanisms that occur on carbon-carbon structure on which a lightning arc is attached.

In that case, the current flows through both the rib and the skin; its typical path is represented with green dashed arrows. The current mainly flows directly in the surface protection, but a significant part of the current may cross the gap between the bolt and the skin or the rib. The intense energy spent in this small resistive gap creates an arc plasma that strongly increases the internal pressure, which blows out in the form of sparks. This mechanism is called "Outgassing" and is considered to be the most important constraint on fasteners. Moreover, in some cases, the electric field may be reinforced between the nut and the rib, and a discharge, called "Thermal spark" may be created. Finally, some discharges may also occur on the edge of composite ribs. This phenomenon, called "Edge Glow" is generally associated with the electric field reinforcement between plies with different orientation.

Sparking simulations

All of the mechanisms associated with sparking phenomena occur during a short time interval ($<1\ \mu s$) and in a small area. Moreover, the sparking location is unpredictable and cannot be accurately determined before the test, as we can see in figure 26. Experiments also bring to light a low repeatability in the results. This could be the reason why advanced characterizations of the plasma associated to sparking phenomena have never been performed or published. The studies are generally based on imaging techniques, electrical characterization and material analyses, which provide some interesting information for the understanding of the sparking phenomena.

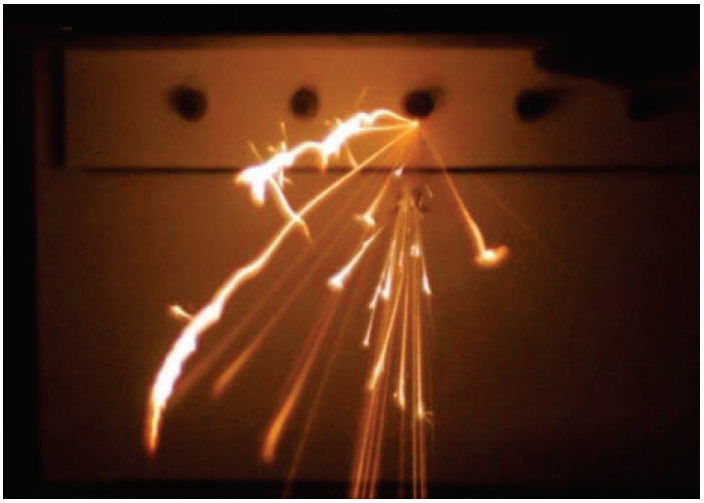

Figure 26 - Picture showing a fastener sparking [30]

Measurements of current distribution into the structures indicate that a significant part of the current may flow into the rib, even if it is initially isolated by insulating layers (sealant or paint) between the skin and the rib, or between the nut and the rib. Rapid breakdowns of dielectric layers may explain the quick transition from insulated to electrically connected rib. Numerical simulations of this mechanism may be performed by taking into account isolating layers and breakdown phenomena (see figure 27).

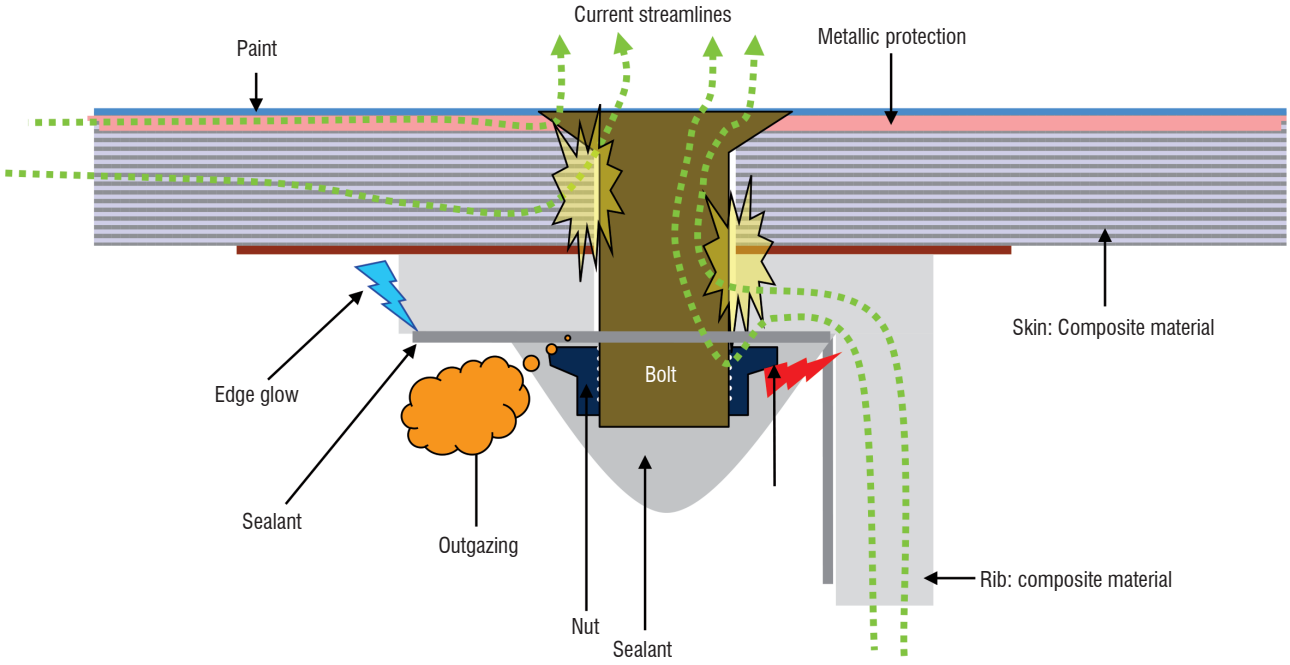

Figure 25 - Schematic drawing of the different mechanisms that occur during sparking phenomenon

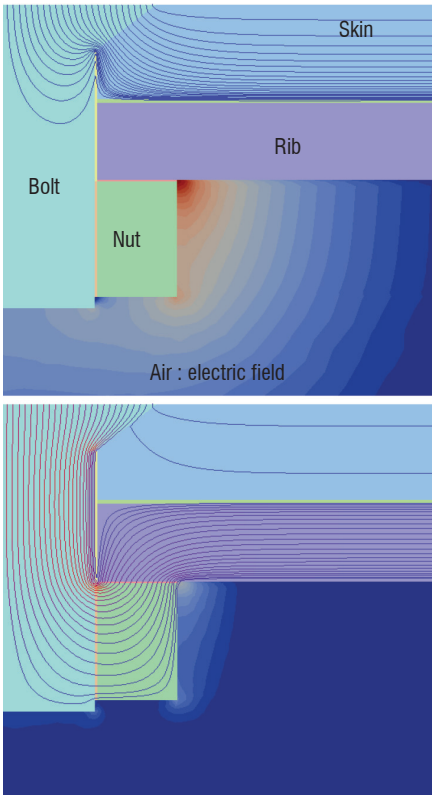

Figure 27 - Current streamlines before and after breakdown of sealant between the nut and the rib. The air zone is colorized with the amplitude of the electric field. The total voltage drop is the same on both situations

On the left hand part of figure 27, the current essentially flows from the head of the bolt to the skin and the resistance between the nut and the rib remains relatively high at this time. We notice an important reinforcement of the electric field close to the nut-rib interface, which leads to a breakdown occurrence. Once this short-circuit has occurred, the current mainly flows through the nut and the rib, and the electric resistance of the assembly decreases. The electric field takes on a relatively low amplitude in relation to the previous state. Some measurements [29] indicate that the presence of metal protection on the surface of the skin is required to restrict most of the current flowing through the rib, by decreasing the skin resistance. Measurements of the resistance of the fasteners before and after a shot indicate significant discrepancies, which may reach a factor of 100. It is generally believed that this changing is associated with melting or welding occurrences in the contact between the different materials.

Arc occurrence in electrical contacts

One of the main physical mechanism involved in the sparking phenomena is associated with the electrical contacts between the different materials used in assemblies. As is shown on the left hand side of figure 28, the real contact area may be very small, because of the surface roughness. Mulazimoglu [30] presented Scanning Electron Microscope (SEM) micrographs showing the micro-structure between a metallic fastener and a carbon fiber composite. Many micro-voids are shown between the metal and the composite structure, which may explain the sparking occurrence during tests. The current density increase may lead to the explosion of the contact spots into the cavity and create important overpressure. Moreover, the electric field in the insulating gaps between the two pieces may give rise to breakdown occurrences of the air or sealant gap, which leads to the fast decrease of the contact resistance in the assembly. Teulet et al. [31] evaluated the internal overpressure due to sealant ablation and arc formation to be about 100 to 450 bars.

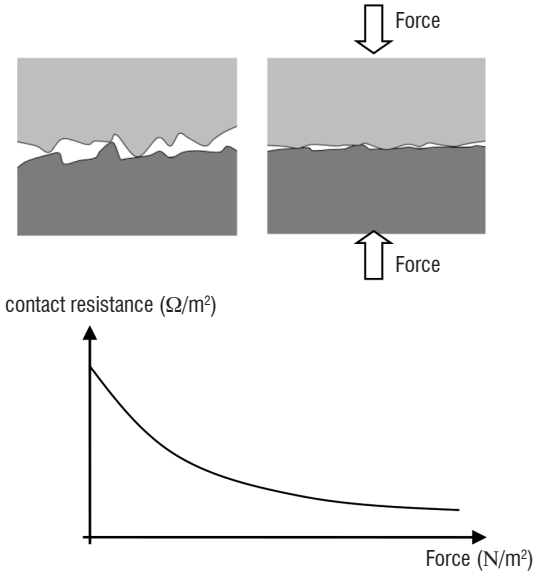

Figure 28 - Schematic drawing of the actual contact area associated with surface irregularities. Right: relationship between contact resistance and the force applied on the contact

One way to reduce the gap and the contact resistance consists in increasing the force into the assembly. The right side of figure 27 shows the typical evolution of the contact resistance between to metallic materials as a function of the pressure. This resistance decreases with pressure, and reaches a minimum value under which the pressure does not act anymore. This feature is quite similar in metal-carbon interfaces. The use of conforming metals that deform into the gap is also a good way to improve contact efficiency. This solution brings the material into intimate electrical contact with the composite structure, which prevents arc and spark formation [30].

Conclusion

The direct lightning effects on aircraft structures are of great importance nowadays, because of the massive use of composite materials in the new generations of aircrafts. In this paper, we have presented the phenomenology of the lightning arc attachment on aircraft. We have shown some differences between lightning arcs observed in flight and those simulated in the laboratory. We have also introduced some recent developments and results from numerical simulations. The shapes, the behaviors and other characteristics are compared with experiments. Discussions on the differences are also presented. In a second section, we have introduced the direct effects of lightning on aircraft skins. Both thermal and mechanical constraints are introduced and illustrated with experimental and numerical results. The negative effects of the paint layer on the damaging of composite and metallic materials have been illustrated. We have finally presented the direct effects of lightning on fasteners in the third section. The main mechanisms that occur during sparking phenomena were presented. Some results available in the literature were also presented and discussed, and we have concluded with the recent solutions to avoid sparking in fasteners and assemblies ■

References

[1] P. LALANDE, A. BONDIOU-CLERGERIE, P. LAROCHE - *Analysis of Available in-Flight Measurements of Lightning Strikes to Aircraft.* Int. Conf. On Lightning and Static Electricity, Toulouse, France (1999)

[2] ARP5412 - *Aircraft Lightning Environment and Related Test Waveforms*. SAE International

[3] F. A. FISHER, J.A. PLUMER, R.A. PERALA - *Lightning Protection of Aircraft*. Lightning Technologies Inc., 1989.

[4] F. HEIDLER, J. M. CVETIC, B. V. STANIC - *Calculation of Lightning Current Parameters.* Power Delivery, IEEE Transactions on, vol. 14, no. 2, pp. 399 –404, Apr. 1999.

[5] V. MAZUR - *Triggered Lightning Strikes to Aircraft and Natural Intracloud Discharges.* Journal of Geophysical Research, Vol 94, N° D3, pp 3311-3325, 1989

[6] I. GALLIMBERTI - *The Mechanism of the Long Spark Formation.* Journal de Physique, Tome 40, 1979.

[7] A. D'ANGOLA, G. COLONNA, C. GORSE, M. CAPITELLI - *Thermodynamic and Transport Properties in Equilibrium Air Plasmas in a Wide Pressure and Temperature Range.* The European Physical Journal D, vol. 46, no. 1, p. 22, 2008.

[8] L. CHEMARTIN, P. LALANDE, E. MONTREUIL, C. DELALONDRE, B. G. CHÉRON, F. LAGO - *Three Dimensional Simulation of a DC Free Burning Arc. Application to Lightning Physics.* Atmospheric Research, vol. 91, pp. 371– 380, Feb. 2009.

[9] M. MODEST - *Radiative Heat Transfer*. Academic Press, 2003.

[10] SIEGEL, HOWELL - *Thermal Radiation Heat Transfer*. 4th ed. Taylor & Francis, 2002

[11] PEYROU, L. CHEMARTIN, P. LALANDE, B.G. CHERON, P. RIVIERE, M.-Y. PERRIN, A. SOUFIANI - *Radiative Properties and Radiative Transfer in High Pressure Thermal Air Plasmas.* J. Phys. D: Appl. Phys. 45 (2012) 000000

[12] SAE ARP 5416, Eurocae ED-105, *Aircraft Lightning Test Methods*, Section 5, 2004

[13] L. CHEMARTIN et al. - *Simulated Lightning Attachment on Unpainted Aluminium Panels During Continuing Current Stage: Effects of the Jet Diverting Electrode.* Pittsfield, Icolse 2009

[14] A. LARSSON, A. BONDIOU-CLERGERIE, P. LALANDE, A. DELANNOY, S. DUPRAZ - *New Methodology for Determining the Extension of Lightning Swept Stroke Zones on Airborne Vehicules.* SAE 2001 transactions, Journal of Aerospace 2001.

[15] A. BIZYAEV et al. - *Investigation of the Sweeping of Lightning in Wind Blown Arc Experiments*. Int. Conf. on Lightning and Static Electricity, Toulouse, 1999

[16] DOBBING, HANSON - *A Swept Stroke Experiment With a Rocket Sled*. Proceeding, International Symposium on electromagnetic Compatibility, Atlanta, 1978

[17] S. TANAKA, K, SUNABE, Y. GODA Y - *Three Dimensional Behaviour Analysis of D.C. Free Arc Column by Image Processing Technique*. XIII Int'l Conf on Gas Discharges and their applications, Glasgow, 2000

[18] HAGENGUTH - *Transactions of the American Institute of Electrical Engineers*, Volume: 68 , Issue: 2, July 1949

[19] A. KADDANI, C. DELALONDRE, O. SIMONIN, H. MINOO - *Thermal and Electrical Coupling of Arc Electrodes*. High Temp. Chem. Processes Vol 3, pp.441,(1994).

[20] S.J. HAIGH - *Impulse Effects during Simulated Lightning Attachments to Lightweight Composite Panels*. International Conference on Lightning and Static Electricity, Paris, 2007

[21] F. LAGO - *Measurements by Stereo Correlation of the Deflexion of Panels Submitted to Lightning Pulse Currents.* International Conference on Lightning and Static Electricity, Oxford, 2011

[22] G. B. WHITHAM - *Linear and Nonlinear Waves* (Pure and Applied Mathematics), 1974

[23] L. CHEMARTIN - PhD, University of Rouen, 2008. http://publications.onera.fr/exl-doc/DOC376449_s1.pdf

[24] A.B. MURPHY - *A Self-Consistent Three-Dimensional Model of the Arc, Electrode and Weld Pool in Gas–Metal Arc Welding.* J. Phys. D: Appl. Phys. 44 (2011) 194009 (11pp)

[25] OGASAWARA et al. - *Coupled Thermal–Electrical Analysis for Carbon Fiber/Epoxy Composites Exposed to Simulated Lightning Current.* Composites Part A 41 (2010) 973–981

[26] P.K. ACKERMAN - *Paint Thickness Comparison Over Composite Lightning Surface Protection Systems and in-Service Ramifications.* Seattle, Icolse 2005

[27] A. Mc KEEMAN BROWN - *Evaluating Surface Protection Systems for Aerospace Composites.* Seattle, Icolse 2005

[28] GINESTE et al. - *Assessment of Lightning Direct Effects Damages by Modelling Techniques*. Pittsfield, Icolse, 2009

[29] REVEL - *Understanding of Sparking Phenomenon in CFRP Assemblies.* Pittsfield, Icolse 2009

[30] MULAZIMOGLU et al. - *Development of Conforming Sleeve Fastener Technology For Lightning Protection of Composite Aircrafts*. Pittsfield, Icolse 2009

[31] TEULET et al. - *Calculation of Pressure Build-up Around Fasteners Due to Sparking*. Oxford, Icolse 2011.

[32] *Aircraft Lightning Environment and Related Test Waveforms Standard.* Issued in August 1997

[33] S. A. WUTZKE, E. PFENDER, E. R. G. ECKERT - *Study of Electric arc Behavior with Superimposed Flow.* AIAA Journal, Vol. 5, No. 4 (1967), pp. 707-713.

AUTHORS

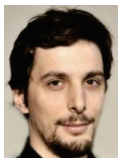

Laurent Chemartin graduated from the Institut National Polythechnique de Grenoble in 2005, and received his Ph.D. degree in 2008 from university of Rouen. His Ph. D. thesis was focused on the modelling and simulation of lighting arc and its interaction with material, in collaboration with EDF and DGA Techniques Aéronautiques. He has been working at Onera as a research engineer since 2009. His main activity is dedicated to the study of direct effects of lighting on aircraft structures. He is currently in charge of the development of a high current generator (GRIFON) for the simulation in laboratory of lighting arcs.

Philippe Lalande graduated from the «Ecole Supérieure de Physique Chimie de Paris" Paris (1992) and received a PhD degree in Plasma Physics from University Paris XI (1996). He joined Onera in 1996 where he has been involved both in the modelling of lightning interaction with aircraft and in the development of onboard atmospheric sensors. He is the Head of the lightning and plasmas Research Unit at Onera Chatillon.

Bruno Peyrou graduated from Ecole Nationale Supérieure d'Ingénieurs de Poitiers in 2008 and received his Ph. D. Degree in 2012 from university of Rouen. His Ph. D. thesis was focused on the development of a lighting arc model dedicated to return stroke. The aim of this work was to simulate the fluid dynamic of arcs subjected to peak of current taking into account the high radiative transfers and the transient electromagnetism phenomenon.

Arnaud Chazottes received an Engineering Diploma from ENSTA in 2005 and a Master degree in Energetic the same year.He joined ONERA in 2007 as icing research scientist in the Physics and Instrumentation department. He has been involved in aircraft and rotorcraft icing for over 4 years, working both on the development and application of several icing codes (2D and 3D). His current activities deal with Atmospheric phenomena modelling and sensor development.

Paul-Quentin Elias graduated from Ecole Centrale Paris in 2003, and hold a Ph. D. from the in Energetics, from the same institution. His main interests are the applications of cold or thermal plasmas to aerospace systems. His current activities involves the development of optical diagnostics for lightning and sliding discharges.

Clarisse Delalondre received the Ph.D. degree in electric arc numerical simulation including non equilibrium sheath modeling from the University of Rouen, France. Since 1990, she has been with Fluid Mechanics, Power Generation and Environment (MFEE) Department, EDF R&D, Chatou, France. She specialized on numerical simulation of electric arc for industrial applications such as welding, arc furnace, plasma torch, circuit breakers, transformer station, and lightning. Her research works focus on nonequilibrium phenomena, unsteady phenomena in electric arc, and developments on electric arc simulations performed in EDF software Code_Saturne®.

Frédéric Lago received his Ph.D. degree in 2004 from the University of Toulouse. His Ph. D. thesis was focused on the modelling of a lighting arc and its interaction with a metallic and composite material, in collaboration with the LAPLACE laboratory and EADS IW. He has been working at DGA Techniques aéronautiques as a lightning expert and test manager since 2007. His main activity is dedicated to the study of direct effects of lighting on aircraft structures. He is in charge of the qualification and certification of aeronautics structure to high current and high voltage directs effects. Frédéric Lago is also a member of the EUROCAE Working Group 31.

Bruno Cheron was born in Rouen on June 16, 1951. He received the degree of Doctor of Physics from the University of Rouen, France in 1979. His thesis was concerned with the Thermodynamic state of an Atmospheric HF Argon Plasma sowed with cadmium. Since 1993, Dr Chéron is Professor of Physics at the University of Rouen. His current research interests include the study of new Plasma Sources, the simulation of Space Shuttle Re-entries, the Treatment of Wastes and the Surface Metrology based on Laser Induced Plasma Spectroscopy.